Controlling the catalytic bond-breaking selectivity of Ni surfaces by step blocking

RONNIE T. VANG[1], KAROLIINA HONKALA[2], SØREN DAHL[3], EBBE K. VESTERGAARD[1], JOACHIM SCHNADT[1], ERIK LÆGSGAARD[1], BJERNE S. CLAUSEN[3], JENS K. NØRSKOV[2] AND FLEMMING BESENBACHER[1]*

[1]Interdisciplinary Nanoscience Center (iNANO), Center for Atomic-scale Materials Physics (CAMP), and Department of Physics and Astronomy, University of Aarhus, DK-8000 Aarhus C, Denmark

[2]Center for Atomic-scale Materials Physics (CAMP), and Department of Physics, Technical University of Denmark, DK-2800 Lyngby, Denmark

[3]Haldor Topsøe A/S, Nymøllevej 55, DK-2800 Lyngby, Denmark

*e-mail: fbe@inano.dk

Published online: 23 January 2005; doi:10.1038/nmat1311

The reactivity of catalytic surfaces is often dominated by very reactive low-coordinated atoms such as step-edge sites[1–11]. However, very little knowledge exists concerning the influence of step edges on the selectivity in reactions involving multiple reaction pathways. Such detailed information could be very valuable in rational design of new catalysts with improved selectivity. Here we show, from an interplay between scanning tunnelling microscopy experiments and density functional theory calculations, that the activation of ethylene on Ni(111) follows the trend of higher reactivity for decomposition at step edges as compared with the higher-coordinated terrace sites. The step-edge effect is considerably more pronounced for the C–C bond breaking than for the C–H bond breaking, and thus steps play an important role in the bond-breaking selectivity. Furthermore, we demonstrate how the number of reactive step sites can be controlled by blocking the steps with Ag. This approach to nanoscale design of catalysts is exploited in the synthesis of a new high-surface-area AgNi alloy catalyst, which is tested in hydrogenolysis experiments.

The idea that special active sites can control the reactivity of an atomic surface dates back to the pioneering work of Taylor[1]. Traditionally, the influence of step edges has been investigated by comparing the reactivity of planar and stepped atomic surfaces, using integrating techniques (for example, reaction rate studies or thermal desorption spectroscopy[2–4]). The scanning tunnelling microscope (STM) with its unique imaging capabilities has proven to be a very powerful tool for identifying the active sites on metal surfaces, as first demonstrated by Ertl and co-workers[5] for NO dissociation on Ru(0001). With the advent of density functional theory (DFT) calculations, it became evident that the difference in

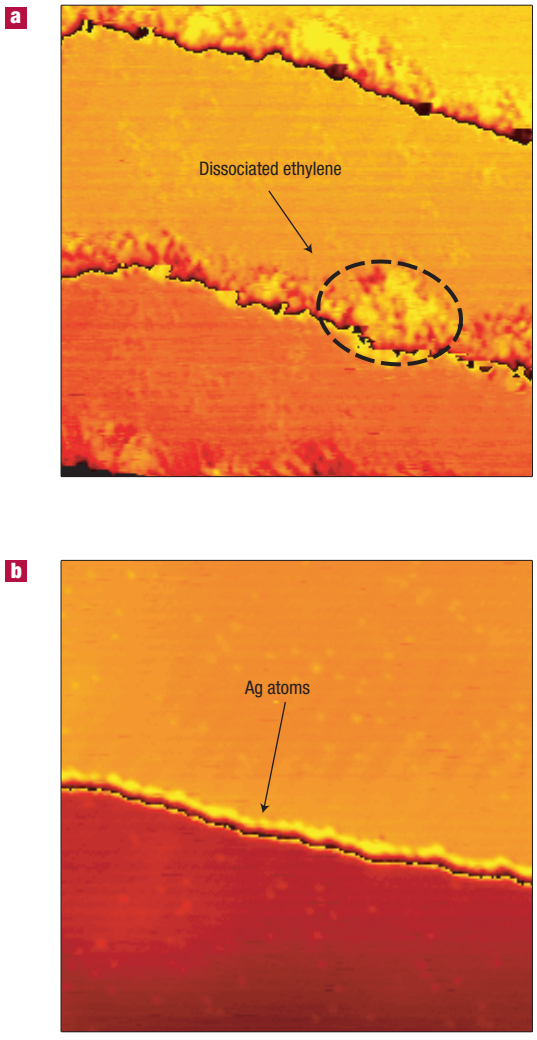

Figure 1 Ethylene decomposition on Ni(111) and Ag/Ni(111). **a**, STM image (200 × 200 Å^2) of a Ni(111) surface after exposure to ethylene (10^{-8} torr; 100 s) at room temperature. A brim of decomposed ethylene is formed along the step edges. **b**, STM image (400 × 400 Å^2) of a Ni(111) surface with the step edges blocked by Ag atoms. No decomposition of ethylene is observed on this modified surface.

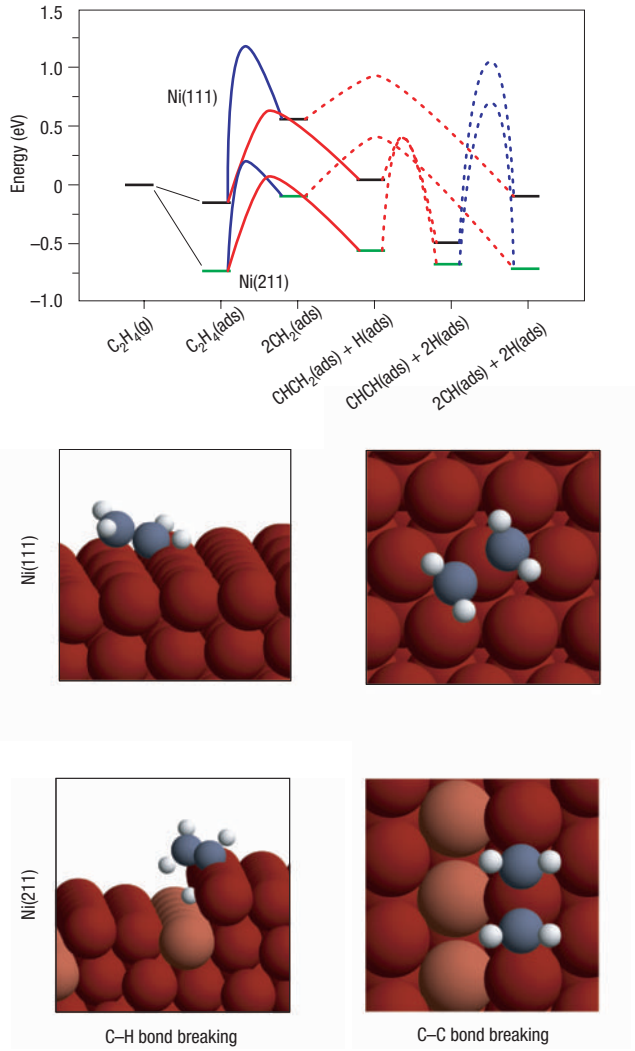

Figure 2 Potential energy diagram for ethylene decomposition on Ni(111) and stepped Ni(211). The diagram shows the activation barriers for C–C bond breaking—dissociation (blue line); and C-H bond breaking—dehydrogenation (red line) on both Ni(111) and Ni(211). The activation barrier for CH_2 dehydrogenation is for one CH_2. The adsorption of different reaction intermediates is marked with black (green) lines on the Ni(111) (Ni(211)) surface. Below, the transition-state structures for dissociation and dehydrogenation are shown on the two different surfaces.

reactivity between terraces and steps can be enormous, and it was confirmed experimentally[6] that the rate of N_2 dissociation is at least nine orders of magnitude larger at steps than on close-packed terraces on Ru(0001) at 500 K. The DFT calculations also showed the effect to be present for a number of other diatomic molecules[7–11]. However, due to the simple structure of the molecules, these studies have only probed the reactivity of the surfaces. It is highly desirable also to have information about the specific role of step edges in reactions for which more than one possible reaction pathway exists. In the present study we have considered the initial step of the decomposition of ethylene (C_2H_4) on Ni(111) in order to gain a detailed knowledge of the influence of the step edges on the rate of C–H and C–C bond breaking. In the end, this bond-breaking selectivity determines the selectivity that can be observed in the macroscopic kinetics—for instance, as the difference in dehydrogenation and hydrogenolysis rates.

Figure 1a shows an STM image of the Ni(111) surface after a 100-s exposure to 10^{-8} torr ethylene at room temperature. The image clearly shows how ethylene has induced a brim with a significantly different corrugation compared with that of the (111) facets along the steps of the surface. The ethylene-induced brim structure was observed exclusively at the upper steps. We never found nucleation of ethylene-induced islands on the terraces of the surface after ethylene exposure. The width of the brim did not increase when the exposure time was increased by a factor of 20, which shows that the process is self-poisoning. As seen from the STM image (Fig. 1a), the self-poisoning is caused by selective adsorption at the step edges, and free step sites are thus needed for the process of forming the brim. If the brim were to be caused by molecularly adsorbed ethylene one would expect the width of the brim to increase with increasing ethylene exposure, which is not consistent with the experimental findings. Furthermore, no brim was observed when the sample was exposed to ethylene at 200 K, indicating that an activation barrier is associated with the formation of the brim. We thus conclude that the formation of the brim is caused by ethylene that has partly or fully decomposed at the step sites.

We calculated the activation barriers for the dissociation (C–C bond breaking) and dehydrogenation (C–H bond breaking) of ethylene both on the flat Ni(111) and the stepped Ni(211) surface. The potential energy diagram is shown in Fig. 2, and from this the binding of ethylene at a step site was found to be favoured by 0.6 eV over binding to a regular terrace site. For all possible intermediates we found adsorption at the upper steps to be the most stable configuration in agreement with the experimental finding. The results showed that the energies of the transition states for ethylene dissociation and dehydrogenation at the steps were both lower by more than 0.5 eV compared with the lowest barrier (dehydrogenation) on the flat Ni(111) surface, thus confirming the high reactivity of the step sites consistent with the present STM findings. Furthermore, the potential-energy diagram showed that the reduction in the height of the activation barrier, when comparing step sites with terrace sites, was considerably more pronounced for dissociation than for dehydrogenation. An indication of the origin of this difference can be obtained by considering the structure of the transition states, see Fig. 2. For C–H bond breaking the transition state is over a single Ni atom both on the (111) surface and at the step. For C–C bond breaking, in contrast, the transition state is somewhat different in the two cases. On the (111) surface, the CH_2 groups end up in the three-fold sites, whereas at the step the final states are the two-fold sites, reflecting the fact that the Ni step-edge atoms are more reactive than those behind the step. The distance between CH_2 in the two-fold sites of the final state at the step is shorter than the distance between the three-fold sites of the final state on the terrace. This means that the CH_2 groups are stabilized at an earlier point on the dissociation path, and the barrier becomes lower. The results in Fig. 2 show that the barriers for C–C and C–H bond breaking for adsorbed ethylene become comparable at the step. We note that the reaction steps following dehydrogenation of C_2H_4 lead to intermediates with larger C–C bond strength, which should result in larger energy barriers for C–C bond breaking. This is illustrated for CH–CH bond breaking in the figure (dotted lines). The main effect of the step is therefore to open C–C bond breaking at the level of adsorbed C_2H_4.

As shown by the DFT calculations, the selectivity of the Ni(111) surface towards ethylene dissociation/dehydrogenation is to a great extent determined by the ratio of the number of steps to terrace atoms, which implies that the selectivity of a Ni(111) surface may be controlled by regulating the availability of free step sites.

Comparison of the dehydrogenation barrier to the higher dissociation barrier on the flat Ni(111) terrace indicates at least partial ethylene dehydrogenation before C–C bond breaking, which

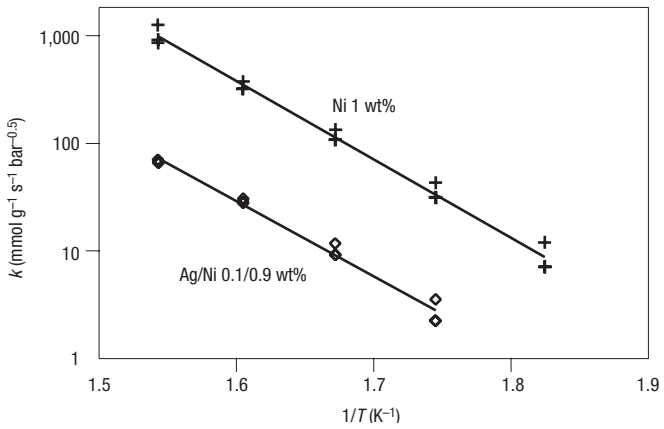

Figure 3 Arrhenius plot of the rate constant for ethane hydrogenolysis over $Ni/MgAl_2O_4$ and $Ag/Ni/MgAl_2O_4$. The rate constant (k) of ethane hydrogenolysis is approximately one order of magnitude lower on $Ag/Ni/MgAl_2O_4$ as compared with $Ni/MgAl_2O_4$, whereas the activation energy (slope of the Arrhenius plot) is similar.

has also been observed experimentally[12]. By blocking the step sites one can thus prevent C–C bond breaking and selectively control the formation of $CHCH_2$.

In order to pursue this strategy we investigated the possibility of blocking the steps by the use of small amounts of Ag, which is known from previous STM studies[13] to nucleate preferentially at the step edges of Ni(111). Figure 1b shows an STM image of a Ni(111) surface after room-temperature deposition of Ag and post-annealing at 800 K. As seen in the STM image, this procedure led to a Ni(111) surface with all step sites being covered by Ag atoms. To demonstrate that Ag does in fact lower the reactivity of the step sites, we subsequently exposed the Ag/Ni sample to 10^{-8} torr ethylene for 100 seconds at room temperature. In this case, no ethylene-induced brim structure was observed at the step edges (or on the terraces). We thus both provided further evidence that the step atoms are the active sites for decomposition of ethylene on the Ni(111) surface at room temperature, and demonstrated the possibility of blocking these sites.

To take the next step and bridge the gap between the fundamental surface science results and applied catalysis, we synthesized a new high-surface-area oxide-supported AgNi alloy catalyst and tested it for the hydrogenolysis of ethane, which is the simplest reaction used to probe the activity for C–C bond breaking (see, for example, ref. 14). Figure 3 summarizes the results of the integral flow-reactor measurements performed on both a pure and a Ag-modified Ni high-surface-area catalyst. From the data, it is evident that the addition of Ag to the Ni catalyst led to a decrease in the rate constant for ethane hydrogenolysis by approximately an order of magnitude. It was, however, also seen that the apparent activation energy (the slope of the curves) was the same for the two catalysts, which strongly indicates that the active sites on the two catalysts are the same. From this observation together with the STM and DFT results we conclude that the decrease in the rate constant was caused by Ag atoms partly covering the Ni step edges. It seems highly plausible that not all step sites are blocked, when taking into account the high degree of complexity of the supported high-surface-area catalyst as compared to the well-defined Ni(111) single-crystal surface on which a complete blocking of all the step sites could be achieved with a relatively low amount of Ag.

In conclusion, we are now closer to a better understanding of the role of step atoms in catalytic processes involving the decomposition of complex molecules. In general, one cannot just simply view the step atoms as more reactive sites but also consider the relative increase in reactivity between different reaction pathways. The step atoms may thus, to a high degree, control the selectivity in a given catalytic process. Such knowledge gained from fundamental surface science experiments could become a powerful tool in the nanoscale design of new and improved catalysts.

METHODS

The STM experiments were conducted in an ultrahigh vacuum (UHV) chamber with the home-built Aarhus STM[15,16]. The sample was exposed to ethylene by backfilling the chamber while the sample was kept at a constant temperature. Subsequently, the sample was transferred to the STM and all STM images were recorded at room temperature.

The spin-polarized DFT calculations were carried out using the dacapo code[17], we used the RPBE[18] generalized gradient correction self-consistently, and the core electrons of all the atoms were treated with Vanderbilt ultrasoft pseudopotentials[19]. All calculations used a six-atom Ni surface unit cell (corresponding to coverage of 1/6) and the equivalent of three Ni(111) layers.

Two different methods were applied to determine the transition states. In some cases the transition state was localized constraining the C–C distances (or C–H distances) and relaxing all other degrees of freedom. In cases, where we did not know the location of the transition state we used the nudged elastic band method[20] to determine the transition state.

The high-surface-area Ni catalyst for the integral flow reactor measurements was prepared by incipient wetness impregnation of an $MgAl_2O_4$ support with $NiNO_3$(aq), and the Ag/Ni catalyst was similarly prepared by incipient wetness impregnation of $AgNO_3$(aq) on the reduced Ni catalyst. Following the impregnation steps the catalysts were dried and subsequently calcined at 450 °C. The metal content in the samples was verified by inductive coupled plasma analysis. The ethane (C_2H_6) hydrogenolysis experiments were performed in an integral plug flow reactor, a U-tube made of quartz, with an inner diameter of 4 mm. The reactor, with a pressure of about 1.0–1.2 bar, was loaded with 200 mg of catalyst, 150–300 μm sieved fraction, which was fixed between two quartz wool wads. Each run started with a reduction of the catalyst in hydrogen (100 ml min^{-1} NTP) at 500 °C for 1 hour. Five different feed-gas compositions were used, 2–3.5% ethane and 15–30% hydrogen in a He flow, at temperatures from 200–400 °C. The conversion was determined by measuring the concentration of methane in the exit gas employing a calibrated mass spectrometer. Methane was the only product detected.

Received 16 June 2004; accepted 1 November 2004; published 23 January 2005.

References

1. Taylor, H. S. A theory of the catalytic surface. *Proc. R. Soc. London Ser. A* **108,** 105–111 (1925).
2. Gwathmey, A. T, Cunningham, R. E The influence of crystal face in catalysis. *Adv. Catal.* **10,** 57–95 (1958).
3. Somorjai, G. A. *Surface Chemistry and Catalysis* (Wiley, New York, 1994).
4. Yates, J. T. Jr, Surface chemistry at metallic step defect sites. *J. Vac. Sci. Technol. A* **13,** 1359–1367 (1995).
5. Zambelli, T., Wintterlinn, J., Trost, J. & Ertl, G. Identification of the "active sites" of a surface-catalyzed reaction. *Science* **273,** 1688–1690 (1996).
6. Dahl, S. *et al.* Role of steps in N_2 activation on Ru(0001). *Phys. Rev. Lett.* **83,** 1814–1817 (1999).
7. Nørskov, J. K. *et al.* Universality in heterogeneous catalysis. *J. Catal.* **209,** 275–278 (2002).
8. Liu, Z. P. & Hu. P. General rules for predicting where a catalytic reaction should occur on metal surfaces: A density functional theory study of C–H and C–O bond breaking/making on flat, stepped, and kinked metal surfaces. *J. Am. Chem. Soc.* **125,** 1958–1967 (2003).
9. Zubkov, T. *et al.* The effect of atomic steps on adsorption and desorption of CO on Ru(109). *Surf. Sci.* **526,** 57–71 (2003).
10. Gambardella, P. *et al.* Oxygen dissociation at Pt steps. *Phys. Rev. Lett.* **87,** 056103 (2001).
11. Ciobîcă, I. M. & van Santen, R. A. Carbon monoxide dissociation on planar and stepped Ru(0001) surfaces. *J. Phys. Chem. B* **107,** 3808–3812 (2003).
12. Lehwald, S. & Ibach, H. Decomposition of hydrocarbons on flat and stepped Ni(111) surfaces. *Surf. Sci.* **89,** 425–445 (1979).
13. Besenbacher, F., Nielsen, L. P. & Sprunger, P. T. in *The Chemical Physics of Solid Surfaces and Heterogeneous Catalysis* Vol. 8 (eds King, D. A. & Woodruff, D. P.) Ch. 10 (Elsevier, Amsterdam, 1997).
14. Sinfelt, J. H. *Bimetallic Catalysts, Discoveries, Concepts, and Applications* (Wiley, New York, 1983).
15. Lægsgaard, E., Besenbacher, F., Mortensen, K. & Stensgaard, I. A fully automated, "thimble-size" scanning tunnelling microscope. *J. Microsc.* **152,** 663–669 (1988).
16. Besenbacher, F. Scanning tunnelling microscopy studies of metal surfaces. *Rep. Prog. Phys.* **59,** 1737–1802 (1996).
17. http://www.fysik.dtu.dk/CAMPOS
18. Hammer, B, Hansen, L. B. & Nørskov, J. K. Improved adsorption energetics within density-functional theory using revised Perdew-Burke-Ernzerhof functionals. *Phys. Rev. B* **59,** 7413–7421 (1999).
19. Vanderbilt D. Soft self-consistent pseudopotentials in a generalized eigenvalue formalism. *Phys. Rev. B* **41,** 7892–7895 (1990).
20. J´onsson, H, Mills, G. & Jacobsen, K. W. in *Classical and Quantum dynamics in Condensed Phase Simulations* (eds Berne, B. J., Ciccotti, G. & Coker, D. F.) Ch. 16 (World Scientific, Singapore, 1998).

Acknowledgements

We acknowledge the financial support from the European Union through the contract HPRN-CT-2002-00170.
Correspondence and requests for materials should be addressed to F. B.

Competing financial interests

The authors declare that they have no competing financial interests.